Article

Journal of
Nanoscience and Nanotechnology
Vol. 19, 7605–7614, 2019
www.aspbs.com/jnn

Improved Performance of Electrochemically Synthesized Polypyrrole Nanofiber Array-Based Amperometric Glucose Biosensor via Crosslinking Technique

Pramila Jakhar, Mayoorika Shukla, and Vipul Singh*

Molecular and Nanoelectronics Research Group (MNRG), Discipline of Electrical Engineering, Indian Institute of Technology Indore, Indore 453552, Madhya Pradesh, India

Herein, we report a novel high sensitivity enzymatic template free glucose biosensor in which enzymes have been immobilized via crosslinking over electropolymerized Polypyrrole nanofiber array (PNA). The nanostructured PPy film was electropolymerized over a Pt-coated glass substrate by the potentiostatic deposition method. Further, the enzyme (GOx) was immobilized over the as-prepared PNA electrode utilizing physical adsorption and crosslinking immobilization method, and the fabricated biosensors were analyzed using amperometric transduction method. The performance of both the types of the biosensor was compared, and further investigations demonstrated the improvement in glucose biosensor response for the electrode utilizing crosslinked GOx. The response time of the prepared biosensor was significantly improved for crosslinked GOx along with nearly six times augmentation in the sensitivity for the same. Among two types of biosensors, the crosslinked electrode based biosensor has shown a high sensitivity of 25.9 mA-cm^{-2}-M^{-1} and an improved response time of ∼30 s with a reasonable linear range of 0.1–2.6 mM which has been reported for the first time via template free electrochemical synthesis approach. The observed results have shown the significant effect of the enzyme immobilization technique on the performance of electrochemical enzymatic glucose biosensor.

Keywords: Template-Free Method, Polypyrrole Nanofiber Array, Cross-Linking, Physical Adsorption.

1. INTRODUCTION

With the increasing demand for glucose biosensors in the food processing industry, clinical diagnostics, and physiological tests, extensive research has been performed for the development of enzymatic biosensor.[1–3] Though non-enzymatic biosensors have also widely been explored for glucose detection however they exhibit poor selectivity towards analyte molecule due to the presence of intermediate oxidizable species.[1] In this regard, enzyme-based glucose biosensors have been proved to be encouraging for glucose detection due to their excellent selectivity and sensitivity. In particular, glucose oxidase (GOx) has been used as a model enzyme for selective glucose determination. It is one of the most widely explored enzymes due to its high catalytic activity and stability.[4] The efficiency and sensitivity of these biosensors can be increased by utilizing nanostructured materials as support matrix having a high surface to volume ratio allowing higher enzyme loading.

The immobilization, i.e. attachment of enzymes to the support matrix is one of the vital steps for fabrication of an enzymatic biosensor. The critical requirement for enzyme immobilization is the support matrix which should provide a biocompatible environment and ensure the proper binding of the enzyme so that it should not leach out. The support matrix having a high surface to volume ratio which provides a microenvironment to enzymes should ensure the stability of enzymes after immobilization and enable electron transfer between enzyme and electrode surface.[5] In this respect, the nanostructures of various conducting polymers (CPs) viz. Polyaniline, Polythiophene, Polypyrrole etc. have been widely accepted as a viable support matrix which can provide higher immobilization sites resulting in higher enzyme loading which in turn leads into higher sensitivity, lower Limit of

*Author to whom correspondence should be addressed.

detection (LOD) and shorter response time of enzymatic glucose biosensors.[5–8] Among several CPs, Polypyrrole is one of the most widely explored polymers for glucose detection due to its excellent electronic conductivity, biocompatibility, and environmental stability.[6,9] The inherent biocompatible property of PPy provides a suitable environment to the enzymes. In addition to this, PPy having low oxidation potential can be easily polymerized by electro-oxidation method (simple, economical) in both aqueous and non-aqueous solutions.[8,10] The most developed nanostructure of PPy reported are nanotubes, nanowire, nanofibers etc.[11,12] Among these especially, PPy nanofibers have gained considerable interest and can be synthesized via electrospinning and electrochemical method.[13,14] Synthesis of PPy nanofibers via electrospinning technique requires the addition of carrier molecules to improve the polymer solution processability which affects the mechanical strength, conductivity, and morphology of grown nanofibers. In addition to this, it has been a challenge to grow defect-free nanofibers with uniform diameters.[11,15] Cetin and camurlu[8] fabricated the PPy nanofibers by chemical vapor polymerization of pyrrole on $FeCl_3$ containing electrospun polyacrylonitrile nanofiber mats. The grown nanofibers average diameter was in the range of 330 to 455 nm. Tavakkol et al.[15] reported the fabrication of Polypyrrole/Poly(vinyl pyrrolidone) nanofibers via electrospinning of pyrrole solution followed by oxidation and discussed the difficulties associated with the electrospinning of PPy due to its low viscosity and solubility. However, PPy nanofibers via electrochemical template-free method can be obtained by simply applying a low oxidation potential to the electrode dipped into an electrolyte solution containing Py monomer. Additionally, the diameter of synthesized nanofibers has been reported to be controlled by means of applied potential, polymerization time, dopant concentration etc.[16]

In the present work, we have utilized a simple, single step, economical, and scalable method for fabrication of PPy nanofibers as an electroactive support matrix for enzymes immobilization. The immobilization of these enzymes onto the support matrix can be performed via various well-known techniques such as physical adsorption, crosslinking, covalent binding, and co-entrapment.[17] In the case of physical adsorption, enzymes are bind to the electrode surface via electrostatic forces between the enzyme and supporting electrode surface. The enzymes are loosely adhered to the electrode surface and can leach out from the matrix due to weak electrostatic forces involved in physical adsorption method. However, immobilization by covalent binding involves modification of support matrix surface by means of a reactive group for attachment of enzymes which provides an efficient binding between enzyme and support matrix material. Another way of immobilization is co-entrapment in which enzymes are mixed with the monomer solution and gets attached to the polymer during polymerization. However, this method requires a huge amount of enzyme for efficient enzyme loading over the support matrix and is also very sensitive to pH of the monomer solution. One of the major drawbacks of this method is that during polymerization the enzymes get buried deep within the polymer matrix causing a reduced response time of the fabricated biosensor due to the delayed interaction between enzyme and substrate molecule.[17–20] Additionally, crosslinking immobilization of the enzyme to the support environment utilizing a crosslinking agent (glutaraldehyde) has been considered a feasible method due to its simplicity and higher enzyme loading.[21] Recently Wang et al.,[3] Elkaoutit et al.,[5] Palod and Singh,[11] Colak et al.[19] have utilized the crosslinking immobilization of GOx and shown the significant influence of this method on the performance of glucose biosensor.

Here, in this work for the first time, we have utilized Polypyrrole nanofibers (electrochemically synthesized via template-free method) as a support matrix to immobilize GOx via crosslinker Glutaraldehyde. In this report, we have utilized physical adsorption and crosslinking immobilization method, and a comparative study of enzyme immobilization techniques on the performance of glucose biosensor has been demonstrated. A stable and biocompatible support matrix of PPy nanofibers for GOx immobilization (microenvironment for enzyme immobilization) has been fabricated using a simple and cost-effective method, i.e. electrochemical deposition method. The enzyme (GOx) immobilization over the PPy nanofibers was performed utilizing physical adsorption and crosslinking immobilization method with the aim of achieving better biosensor performance. The immobilization via crosslinking has been optimized to load Bovine serum albumin (BSA), glutaraldehyde, and subsequently GOx onto the support matrix. Further, the two types of fabricated biosensors were analyzed using amperometric detection method and the immobilization methods have shown the significant impact on the biosensor performance.

2. EXPERIMENTAL DETAILS

2.1. Chemicals

Pyrrole monomer (C_4H_5N), Lithium perchlorate ($LiClO_4$), Sodium phosphate monobasic (NaH_2PO_4), Sodium phosphate dibasic (Na_2HPO_4), Potassium ferricyanide/ferrocyanide $[Fe(CN)_6]^{3-/4-}$, D-(+)-glucose, L-ascorbic acid, Uric acid, Glucose oxidase (GOx) with specific activity of 166 U/mg (specified by manufacturer) from Aspergillus niger (E. C. 1.1.3.4), Bovine serum albumin (BSA) and Glutaraldehyde were obtained from Sigma-Aldrich. All the chemicals used were of analytical grade. All aqueous solutions were prepared using Deionized water (DI) of 18 MΩ resistivity. 0.1 M Phosphate buffer solution (PBS) with pH 6.8 was prepared using NaH_2PO_4, Na_2HPO_4 and deionized (DI) water. 1M glucose stock

solution was prepared in DI and kept for mutarotation (24 hr) to establish the equilibrium between α and β anomers.

2.2. Preparation of PNA Electrode and Characterization

Primarily, the glass substrates (1 cm × 1 cm) were cleaned by ultrasonication in acetone, isopropanol for 10 min followed by DI water for 5 min. Finally, the ultrasonically cleaned glass substrates were treated by Radio Corporation of America (RCA) clean-1 process for the hydrophilic glass surface. Further, Pt (50 nm) with an intermediate layer of chromium (5 nm) (to improve the adhesion of Pt on glass) was deposited over the cleaned glass substrates using dc magnetron sputtering at a base pressure of 1×10^{-6} mbar and a working pressure of 3 mTorr.[22] The continuous flow of Ar gas was maintained at 10 standard cubic centimeter per minute (sccm) during Pt deposition. Furthermore, Polypyrrole was deposited over the Pt-coated glass substrate using electropolymerization method. For electropolymerization, Pyrrole (Py) was distilled at 130° C, and the electrolyte solution of 0.1 M Py, 1–70 mM $LiClO_4$ with 0.1 M PBS (pH 6.8) was prepared as reported in our previous work.[23] According to the optimized growth conditions the best performing electrode corresponding to 70 mM $LiClO_4$ concentration has been taken for further improvement in the biosensor performance. The schematic illustration of biosensor fabrication has been represented in Figure 1. Briefly, the electrochemical deposition of Polypyrrole was carried out using electrochemical workstation Autolab PGSTAT302N having three-electrode cell configuration. The cell consisted of electrolyte solution of 0.1 M Py monomer, 70 mM $LiClO_4$ in 0.1 PBS (pH-6.8) where platinum coated glass substrate, Ag/AgCl electrode, and platinum foil have been utilized as working, reference, and counter electrode respectively. A constant potential (0.85 V) was applied to the working electrode for 3600 s to obtain PNA over a Pt-coated glass substrate. The morphology of electrosynthesized Polypyrrole was determined using Field Emission Scanning Electron Microscopy (FESEM, Carl Zeiss SUPRA55). Further, Glucose oxidase (GOx) was immobilized over the fabricated Glass/Cr-Pt/PNA electrode using physical adsorption and crosslinking immobilization technique. The immobilization of GOx was confirmed by Fourier Transform Infra-red Spectroscopy (FTIR) and Electrochemical Impedance Spectroscopy (EIS) for both types of electrodes. The amount of GOx loaded onto the electrode for both the cases was determined using Fluorescence spectra obtained from FluoroMax-4p spectrofluorometer from Horiba Jobin Yvon (Model: FM-100). Furthermore, the as-fabricated biosensors were characterized using cyclic voltammetry and amperometric method. All the current measurements were executed using electrochemical workstation Autolab PGSTAT302N.

2.3. Modification of PNA Electrode with GOx and Its Quantification

The immobilization of GOx (specific activity of 166 U/mg) onto the fabricated electrode was performed using physical adsorption and crosslinking immobilization techniques. Firstly, GOx was physically adsorbed onto the prepared electrode (area = 0.15 cm^2). This is the simplest method of enzyme immobilization in which enzyme binds to the electrode surface via electrostatic interaction utilizing the positive charge on PPy. In physical adsorption process, GOx aliquot (10 μL) from a stock solution of 10 mg/mL prepared in 0.1 M PBS was dropped onto the fabricated PNA electrode and was kept in an incubator at 4° C temperature. However, for crosslinking immobilization method, GOx was crosslinked over the PNA electrode surface via glutaraldehyde, which has been used as a crosslinker. A mixture of 10 mg/mL bovine serum albumin (BSA) (acting as a stabilizer for GOx)[11] and 20 μL glutaraldehyde (crosslinking agent) was prepared in 1 mL PBS, and 10 μL aliquot of this mixture solution was drop cast over the as-prepared electrode. After drying the electrode at room temperature, 10 μL aliquots of GOx was immobilized over it and kept in an incubator at 4° C temperature. Both the types of electrodes were washed into PBS to remove loosely adhered GOx molecules. Further, this PBS solution was utilized for the estimation of GOx molecules attached to both electrode surfaces.

Each GOx molecule has an aromatic residue named tryptophan, which shows an intrinsic fluorescence in GOx. Therefore, when the solution having GOx molecule is excited at 280 nm, it contributes to fluorescence emission

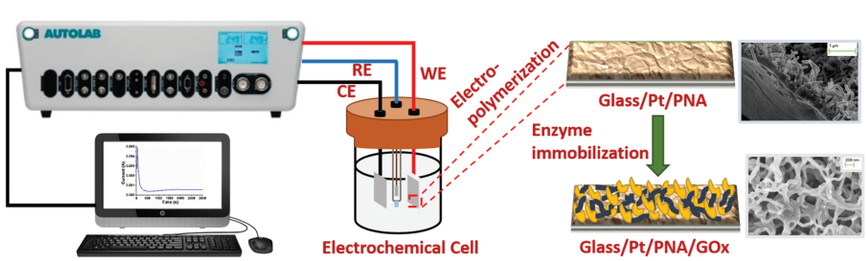

Figure 1. Schematic illustration of biosensor fabrication via electrochemical polymerization method.

at 330 nm. The intensity of fluorescence emission at 330 nm is directly related to GOx concentration in the solution.[24] Henceforth the optical characteristic of the GOx molecule has been utilized to evaluate the amount of enzyme loaded over the PNA support matrix. A linear calibration curve corresponding to the known amount of GOx in 0.1 M PBS and its fluorescence intensity was obtained. Further, fluorescence intensity was measured for PBS containing unadhered GOx molecules for both the electrodes. Finally, the amount of unadhered GOx was estimated by using the calibration curve and the fluorescence intensity corresponding to unadhered GOx molecules. Thus the amount of enzyme immobilized over each electrode was determined by taking the difference of the known amount of enzyme immobilized (100 μg) and the calculated unadhered enzymes.

2.4. Amperometric Detection of Glucose

Amperometric detection of glucose was carried out in a three electrode electrochemical cell using both the types of electrodes as the working electrode. All the current measurements were performed at a constant potential of 0.7 V applied to the working electrode immersed in continuously stirred 0.1 M PBS (pH 6.8). Successively glucose aliquots were injected into the electrolyte solution after the steady-state current value was reached. When glucose is added into the electrolyte solution, GOx attached to PNA electrode catalyzes the oxidation of glucose into gluconic acid, and GOx itself gets reduced in the redox reaction. After that, reduced GOx, i.e., GOx(red) gets oxidized back into its original form by oxygen present in solution releasing H_2O_2 as a byproduct. The produced H_2O_2 decomposes into electrons and ions with the application of a potential, which provides a measure of glucose added to the solution. The mechanism of glucose detection has been presented in Eqs. (1)–(3).

$$C_6H_{12}O_6 + GOx(oxd) + H_2O \rightarrow C_6H_{12}O_7 + GOx(red) \quad (1)$$

$$GOx(red) + O_2 \rightarrow GOx(oxd) + H_2O_2 \quad (2)$$

$$H_2O_2 \xrightarrow{0.7\ V} 2H^+ + 2e^- + O_2 \quad (3)$$

Thus as indicated in Eqs. (1)–(3), with the addition of glucose current increases due to the generation of electrons. Current responses were recorded for both types of as prepared electrodes with successive addition of glucose. The calibration curve was obtained using the steady-state current density values corresponding to each glucose concentration. All figure of merits of biosensor viz. sensitivity, linear range, and response time were calculated by calibration plot.

3. RESULTS AND DISCUSSION

3.1. Morphological Characterization

The morphology of as-prepared PNA electrode synthesized at a potential of 0.85 V in an electrolyte solution of 0.1 M Py, 70 mM $LiCO_4$, and 0.1 M PBS was determined using FESEM. Figures 2(a), (b) shows the top view FESEM image and the diameter distribution of PNA electrode respectively. The inset shows the magnified view of the grown nanofibers of PNA electrode synthesized in an electrolyte solution of 0.1 M Py, 70 mM $LiClO_4$ and 0.1 M PBS at 0.85 V potential. As evident from the FESEM images that high-density uniform nanofibers growth have been observed over a large area for the optimized growth conditions. The synthesized nanofibers were longer as compared to the diameter which shows higher aspect ratio of the obtained nanofibers, as clear from Figure 2(a). The nanofibrous growth with improved aspect ratio ensures less hindered charge transport, high specific surface area and thus higher enzyme loading which directly influences the biosensor figure of merits.[25] Figure 2(b) shows the histogram plot of diameter distribution of grown nanofibers. The diameter distribution of nanofibers was obtained from FESEM images by randomly selecting 30 nanofibers using "imtool" of MATLAB, and it was estimated to be in a range of 150–200 nm. The FESEM image clearly shows the porous and homogeneously distributed nanofibers morphology having a high surface area which is beneficial for higher enzyme loading.

3.2. Enzyme Immobilization and Quantification

Enzyme (GOx) is a protein which comprises a number of amino acids. These amino acids have been reported to be arranged into helices, turns, and sheets which account for the complex structures and activity of enzymes.[4] The structure and activity of GOx are very much sensitive to the microenvironment of the GOx. Thus, the structural analysis of GOx was performed using FTIR spectroscopy after the immobilization of GOx. FTIR study has been utilized to analyze the effect of immobilization methods on the conformational changes in the structure of GOx. FTIR of PNA, native GOx and immobilized GOx was performed to confirm the immobilization of GOx. The changes in the structure of GOx after immobilization onto PNA electrode was studied with respect to FTIR of native GOx. In FTIR spectra of protein, the amide group, amide I (1700–1600 cm^{-1}) and amide II (1600–1500 cm^{-1}) have been observed to be very much sensitive to protein conformation.[11] Figure 3(a) shows the FTIR spectra of as-prepared PNA. The spectra of PNA showed the significant peaks at 3571 cm^{-1} and 3428 cm^{-1} which can be attributed to amine N–H stretching, peaks at 1627 cm^{-1} and 1449 cm^{-1} indicates C=C and C–C stretching respectively. In addition, peak at 1074 cm^{-1} assigned to N–H and C–H aromatic in-plane bending. Furthermore, peaks at 705 cm^{-1} and 613 cm^{-1} corresponded to C–H and C–C out of plane deformation in heterocyclic aromatic rings of polymeric conjugation in PPy which was in good agreement with the literature.[21,26] The FTIR spectra of native GOx and immobilized GOx via

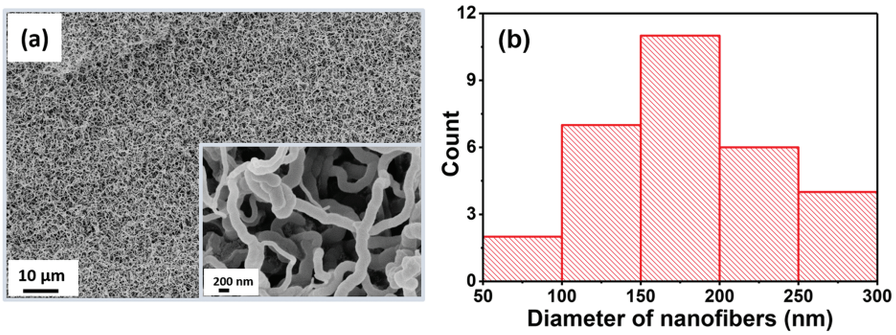

Figure 2. (a) FESEM image of PNA prepared in an electrolyte solution of 0.1 M Py, 70 mM $LiClO_4$ into 0.1 M PBS (pH-6.8) at a potential of 0.85 V versus Ag/AgCl. The inset shows the magnified view of the same (b) Diameter distribution of randomly selected nanofibers from FESEM image.

physical adsorption and cross-linking has been shown in Figure 3(b). The FTIR spectra for native GOx has shown two characteristics amide bands: amide I and amide II centered at around 1645 cm^{-1} and 1543 cm^{-1} respectively. The amide I band at 1654 cm^{-1} corresponds to –C═O stretching vibration while amide II at 1543 cm^{-1} relates to N–H in-plane bending.[21] Figure 3(b) shows that for both the type of immobilization methods the absorption bands (amide I and amide II) have been found at the same peaks as that of native GOx which confirm the proper immobilization of GOx with its retained activity. Additionally, the cross-linking immobilization has shown higher intensity in FTIR spectra as compared to physical adsorption which has demonstrated higher enzyme loading for crosslinked GOx. Further to obtain quantitative information of secondary structure elements of the GOx, amide I peak was analyzed. Deconvolution of amide I band ranging from 1600–1700 cm^{-1} was performed using Voigt function. The peak positions in spectra were determined using minima of second derivative spectra of amide I region. Deconvoluted peaks in amide I spectra of native, physically adsorbed and crosslinked GOx were fitted to a cumulative peak obtained same as original spectra for all. The deconvoluted spectra of native, physically adsorbed, and crosslinked GOx has been shown in Figures 4(a)–(c). The bands at 1650–1660 cm^{-1}, 1620–1640 cm^{-1}, and 1660–1685 cm^{-1} have been designated to α-helix, β-sheets, and β-turns respectively. Moreover, the bands at 1610–1620 cm^{-1} and 1685–1695 cm^{-1} have been assigned to antiparallel β-sheets and bands at 1640–1650 cm^{-1} were referred to random coils present in GOx structure.[27] The percent of the individual secondary element was determined by dividing the area of each band to the total area of amide I. The reckoned secondary structure elements of GOx in different microenvironments have been presented in Figure 4(d). The secondary structure conformation of native GOx has shown ∼28% α-helix, ∼33% β-sheets, ∼35% β-turns, and ∼4% antiparallel β-sheets. However, after physical adsorption of GOx, α-helix and β-sheets were reduced to ∼24% and ∼23% respectively. There was no significant change in β-turns (∼34%). Additionally, the antiparallel β-sheets were found to increase up to ∼19% for physically adsorbed GOx. The crosslinking immobilization of GOx has revealed ∼23% α-helix, ∼23% β-sheets, ∼30% β-turns, ∼4% antiparallel β-sheets, and ∼20% random coils. The obtained percent changes in the secondary structure elements α-helix and β-sheet were related to the GOx's activity. With physical adsorption and crosslinking immobilization of GOx, conformational changes in the secondary structure of GOx has been found to vary as compared to native GOx. Regardless of the changes in the percentage of secondary structure

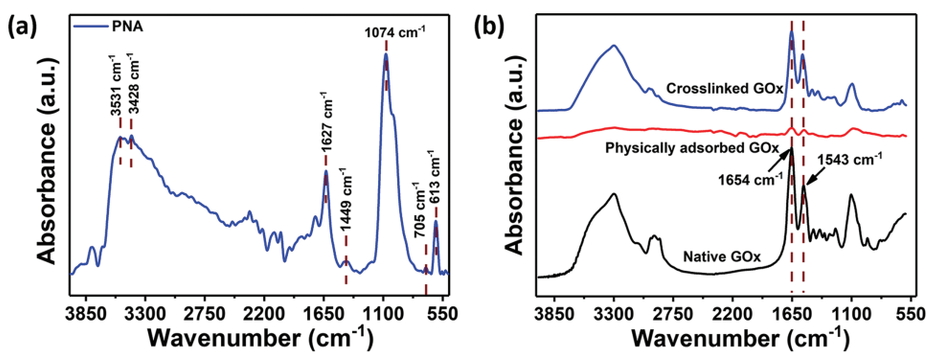

Figure 3. FTIR spectra of (a) as-prepared PNA electrode (b) Native GOx, Physically adsorbed and crosslinked GOx.

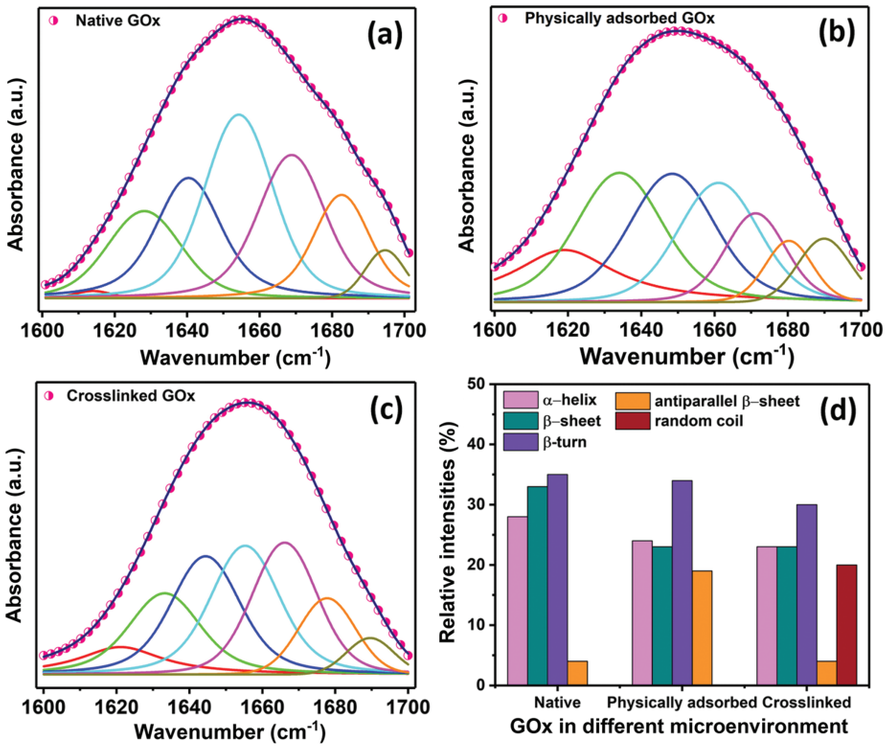

Figure 4. Deconvolution of amide I spectra of (a) Native (b) Physically adsorbed, and (c) crosslinked GOx (d) Relative amount of secondary structure elements of GOx for all different microenvironments (Native, Physically adsorbed, and crosslinked GOx) calculated from deconvolution of amide I spectra.

elements after immobilization of GOx, the presence of α-helix and β-sheets defines the retained activity of GOx.

Further, the immobilization of GOx was confirmed by EIS which was related to the impedance changes on surface modification of PNA with GOx. EIS was performed in 0.1 M PBS with pH-6.8 consisting of 5 mM redox couple, i.e., $K_3Fe(CN)_6$ and $K_4Fe(CN)_6$. A small ac input signal of 10 mV amplitude with frequency varying from 100 kHz to 0.1 Hz was applied to the electrode for recording impedance spectra. The obtained impedance spectra of bare Pt and modified electrodes have been shown in Figure 5. The impedance spectra presented in Nyquist plot consist of a semicircle part at the higher frequency and a linear part in the lower frequency region. The observed Nyquist plots for all the electrodes were related to the interfacial behavior of each electrode. The semicircle region and the linear region correspond to the electron transfer limited processes and diffusion limiting processes respectively. The semicircle diameter represents the electron transfer resistance experienced by redox couple at the electrode and electrolyte interface which relates to the conductivity of the modified electrode.[26] The obtained impedance spectra for each modified electrode was fitted to an equivalent electrical circuit of R(Q(Rs(Q(R_{ct}W)))) using ZSimpWin 3.2 impedance software. Where R_{ct} defines the charge transfer resistance value. As shown in Figure 5 upon immobilization of GOx, the semicircle diameter has been found to increase for both the immobilization processes as compared to PNA electrode. The increment in the R_{ct} value from 350 Ω to 1201 Ω and 1918 Ω was obtained after the modification of PNA electrode for physically adsorbed and crosslinked GOx respectively. The decrease in the conductivity of physically adsorbed and crosslinked GOx electrode as compared to

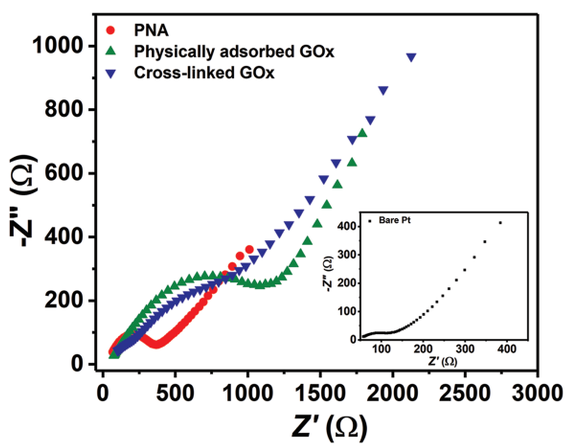

Figure 5. Nyquist plot of Bare Pt, PNA, physically adsorbed and crosslinked GOx over PNA.

PNA after immobilization of GOx was due to the non-conductive behavior of GOx.[28] The observed increment in charge transfer resistance after the immobilization of GOx onto PNA electrode confirms the immobilization of GOx for both the type of immobilization methods.[29]

Furthermore, for both the type of immobilization, the amount of enzyme loaded over PNA electrode was calculated by Fluorescence utilizing the optical property of Tryptophan present in GOx.[11] In case of physical adsorption, the GOx binds to PPy via electrostatic interaction between polycationic PPy and GOx while in crosslinking method GOx binds to the surface of PPy via a covalent bond between an amino group of enzyme and PNA via the crosslinker glutaraldehyde. When GOx is immobilized onto functionalized PPy support matrix, one aldehyde group of glutaraldehyde reacts with the primary amino group of GOx and the other aldehyde group of crosslinker binds with the amino group of BSA and PPy support matrix.[3, 34]

The as-fabricated PNA electrode has high-density nanofibers having a higher surface area which can provide higher enzyme loading. The loading mainly depends on the surface area and the method of enzyme immobilization. The amount of GOx loaded over PNA was found ~559 μg-cm^{-2} and ~642 μg-cm^{-2} for physical adsorption and crosslinking immobilization respectively which depicts that the crosslinking immobilization has facilitated higher enzyme loading which was in good agreement with the observations of FTIR spectra. The higher enzyme loading is a prerequisite for improved sensitivity of the biosensor.

3.3. Cyclic Voltammetry Analysis

To study the catalytic activity of GOx towards glucose oxidation, cyclic voltammetry of both the as-prepared biosensors was performed in 0.1 M PBS (pH-6.8) without stirring. Figure 6(a) shows the cyclic voltammogram of the crosslinked electrode, where the potential applied to the working electrode was swept from 0 to 0.7 V at a scan rate of 100 mV/s. The CV shows the electrode behavior without glucose and with the subsequent addition of glucose. With the injection of glucose to the electrolyte solution, a sharp increase in the anodic current was observed as compared to the current obtained without glucose, validating the activity of GOx immobilized onto PNA. The crosslinked PNA electrode has shown the current increment up to 3 mM glucose concentration. The observed current rise suggests the glucose oxidation catalyzed by GOx. Figure 6(b) represents the comparison between CV responses of physical adsorption and crosslinked GOx based electrodes with the addition of 3 mM glucose concentration. As evident from Figure 6(b) the oxidation current values has been significantly enhanced for crosslinked GOx as compared to physically adsorbed GOx. The observed current increment for crosslinked GOx based electrode was correlated with higher enzyme loading in case of crosslinking immobilization as compared to physical adsorption which was evident from enzyme loading estimation. Further to confirm the observed results amperometric detection of glucose was carried out for both the types of electrodes.

3.4. Amperometric Detection of Glucose

The as-fabricated two types of biosensors were analyzed using amperometric detection method. Amperometric response of both the biosensors prepared by using physical adsorption and crosslinking immobilization methods have been presented in Figure 7(a). The current response of the fabricated biosensors showed an instantaneous increment in the current upon injection of glucose representing the rate of oxidation of glucose. The immediate rise in the current indicates toward the retained catalytic activity of the enzyme, after immobilization on PNA electrode as also visible from CV. In case of physical adsorption firstly 0.1 mM glucose was injected with the successive addition of 0.25 mM, 0.5 mM, and 1 mM glucose at every 70 s showing the corresponding rise in the current density and a step-like response has been obtained as evident from Figure 7(a). Additionally, the amperometric response of crosslinked GOx over PNA has also

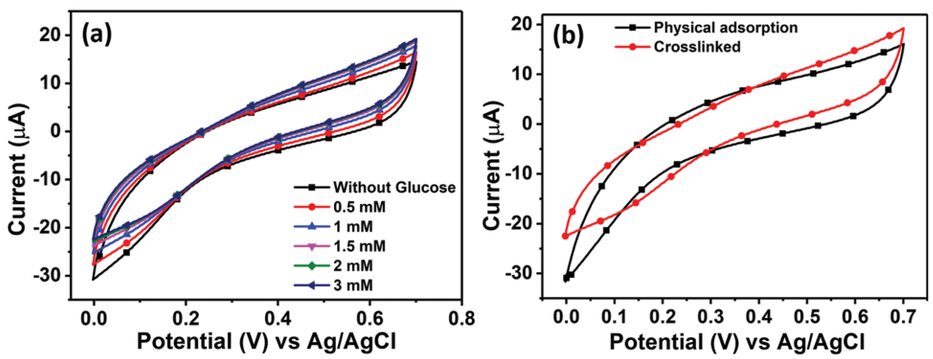

Figure 6. Cyclic voltammogram of (a) PNA with crosslinked GOx (b) Comparison of physically adsorbed GOx and crosslinked GOx onto PNA with the injection of 3 mM glucose recorded in 0.1 M PBS at a scan rate of 100 mV/s.

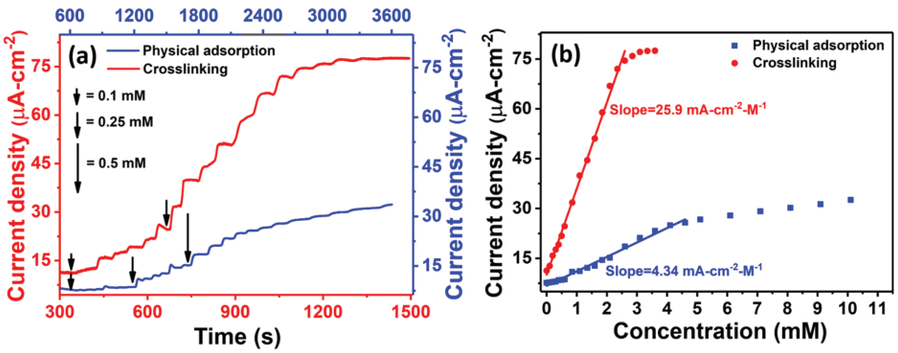

Figure 7. (a) Amperometric responses (b) Calibration curves of biosensors fabricated utilizing Physical adsorption and crosslinking immobilization of GOx.

shown the step-like response with the successive addition of 0.1 mM glucose followed by 0.25 mM glucose at every 50 s. The calibration plots of both the biosensors were obtained from the corresponding amperometric responses, and the performance of both the biosensors was compared as shown in Figure 7(b). The calibration curves of both the biosensors follow the enzyme kinetics. For physical adsorption, initially at the lower concentrations of glucose up to 4.6 mM, the current density has increased linearly. Further increase in the glucose concentration has led to saturation in the current density. The linear range corresponds to the fact that active sites of the enzyme are still available for the redox reaction. However, the saturation region observed at the higher concentration of glucose represents that all the active sites of the enzymes have been occupied by the glucose molecules. After the saturation region, no further increment in the current was observed with the addition of glucose. The sensitivity of the obtained biosensors was defined as the slope of the calibration curve for linear range, and the calculated value of sensitivity was observed as 4.34 mA-cm^{-2}-M^{-1} with a linear range of 0.1–4.6 mM for physically adsorbed GOx based biosensor. However, the improved sensitivity of 25.9 mA-cm^{-2}-M^{-1} was obtained by incorporating the crosslinked GOx as noticeable from Figure 7(b). The linear range of detection for crosslinked GOx based electrode was estimated to be 0.1–2.6 mM. In addition to sensitivity and linear range of detection, the response time for each biosensor was defined as the time taken to reach 90% of the steady state current value which was calculated to be approximately 45 s and 30 s for the biosensors prepared by physical adsorption and crosslinking immobilization techniques respectively. The observed improvement in the performance of crosslinked GOx based biosensor was ascribed to increased enzyme loading due to cross-linking immobilization of GOx. Cross-linking technique incorporates the higher amount of enzyme over the support matrix due to the covalent bond formation with a cross-linker. A comparison of all figure of merits of both the prepared biosensors has been illustrated in Table I. Furthermore, Table II shows the comparison of all figure of merits of the best performing biosensor with some previously reported work where different PPy nanostructures have been employed as a support matrix for GOx immobilization.

The immobilization methods have shown significant influence on the sensitivity and linear range of operation of the glucose biosensor. With the crosslinked GOx the sensitivity of the glucose biosensor was improved drastically. Although, the linear range of the presented glucose biosensor with crosslinking was observed to be narrower. Thus, the measurement of glucose in the human blood sample using proposed biosensor can be performed by the dilution of the blood sample. Moreover, the crosslinked GOx based glucose biosensor with the linear range of 0.1–2.6 mM can find application for noninvasive glucose detection in human body fluids such as sweat and saliva.[32, 33]

3.5. Interference Effect Study, Reproducibility, and Real Blood Sample Analysis

In addition to glucose, human blood and serum contain several other electroactive species viz. uric acid, ascorbic acid, etc. which also gets easily oxidized at 0.7 V potential. Thus these electroactive species may also interfere with the biosensor response during glucose detection.[31] Hence, it is required to define the anti-interference capability of the biosensor for obtaining a practical glucose biosensor. Here, the effect of interfering species; ascorbic acid (0.1 mM) and uric acid (0.4 mM) was examined on the performance of as-prepared glucose biosensor. To study the influence of interferents' initially 0.25 mM glucose was introduced into the cell and allowed to reach a steady state. Afterwards, sequentially 0.1 mM ascorbic

Table I. Comparison of prepared electrodes using physical adsorption and crosslinking immobilization of GOx.

Electrode	Sensitivity (mA-cm^{-2}-M^{-1})	Linear range (mM)	Response time (s)
Physical adsorption of GOx	4.34	0.1–4.6	~45
Crosslinked GOx	25.9	0.1–2.6	~30

Table II. Comparison of the proposed biosensor performance with some recently reported work.

S. No.	Electrode	Sensitivity ($mA\text{-}cm^{-2}\text{-}M^{-1}$)	Linear range (mM)	Response time (s)	Ref.
1	Glass/Cr-Pt/PNA/GOx	25.9	0.1–2.6	∼30	This work
2	Pt/PPy-PVS/GOx	—	0.05–1	200	[19]
3	Glass/Au/PPy/GOx	1.9	0.125–11.25	30–35	[13]
4	Pt/PPy/GOx	0.22	0–10	15	[30]

acid and 0.4 mM uric acid was injected into the electrolyte solution. Figure 8 shows the interference effect on sensing response of crosslinked immobilized GOx onto PNA electrode. The current response shows the similar behavior of biosensor, and an increase of 0.36% and 3.7% in the current density corresponding to ascorbic acid and uric acid respectively was observed. Figure 8 presents that, the biosensor has shown a very less current rise as compared to glucose which specifies the anti-interference capability of biosensor owing to the high specificity and selectivity of enzymes towards glucose.

Moreover, the reproducibility of the as-fabricated crosslinked GOx based biosensor was determined. The amperometric responses of three similarly prepared biosensors were compared, and a relative standard deviation of 6.6% was obtained which was found to be in an acceptable range. Furthermore, to check the reliability of as-fabricated biosensor for practical application real whole blood sample was taken. The freshly taken whole blood sample was injected into the electrochemical cell consisting of PBS, and the current rise was observed relating to the glucose concentration which was compared with the glucose concentration measured by standard GOD-POD colorimetric assay[23] and was observed to be 5.5 mM. The estimated value of glucose concentration by as-fabricated biosensor was 5.1 mM with a deviation of 7.2% which was in good agreement with the glucose concentration measured by standard glucose assay.

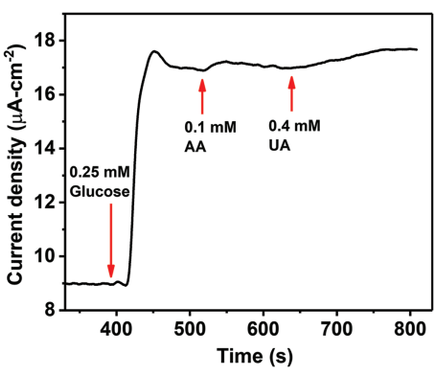

Figure 8. Interference effect of ascorbic acid and uric acid on the performance of crosslinked GOx biosensor.

4. CONCLUSION

In summary, an enzymatic glucose biosensor based on Ppy nanofibers has been fabricated successfully. The PNA electrode has been employed as a support matrix for GOx immobilization. The immobilization matrix, i.e., PNA electrode has provided a biocompatible environment to GOx. The immobilization of GOx has been performed via physical adsorption, and crosslinking method and the performance of both types of biosensor has been evaluated and compared. The incorporation of crosslinked GOx via glutaraldehyde (cross-linker) has resulted in six times enhancement in the sensitivity along with improved response time. The biosensor has shown the sensitivity of 4.34 $mA\text{-}cm^{-2}\text{-}M^{-1}$ with a linear range of 0.1- 4.6 mM and response time of 45 s for physically adsorbed GOx while 25.9 $mA\text{-}cm^{-2}\text{-}M^{-1}$ with a linear range and response time of 0.1–2.6 mM and ∼30 s respectively for crosslinked GOx. The biosensor fabricated with the crosslinked GOx has shown the increased enzyme loading as compared to physically adsorbed GOx leading to an enhanced sensitivity of the prepared biosensor. The observed results have shown that the selection of immobilization technique plays a significant role in the performance of biosensors as it directly affects the enzyme loading which is one of the vital aspects that is responsible for the improvement in biosensors performance.

Acknowledgments: One of the authors Pramila is grateful to Sophisticated Instrument Centre, IIT Indore for providing FESEM, Fluorescence and Potentiostat/Galvanostat facilities. Pramila would also like to thank Dr. Mukul Gupta (University Grants Commission Department of Atomic Energy (UGC DAE) Consortium for Scientific Research Indore (M. P.), India) for the usage of the DC magnetron sputtering system. Pramila would like to thank Dr. Parasharam M. Shirage (Associate Professor, Discipline of Metallurgy Engineering and Materials Science IIT Indore) for providing access to Potentiostat/Galvanostat for EIS. Pramila would further like to thank the Ministry of Human Resource and Development (MHRD), India for providing the Teaching Assistantship (TA). Author, V. S. would like to thank Director of IIT Indore for providing his constant support and encouragement for research.

References and Notes

1. L. Wang, L. Miao, H. Yang, J. Yu, Y. Xie, L. Xu, and Y. Song, *Sens. Actuators B Chem.* 253, 108 (**2017**).
2. M. F. Hossain and J. Y. Park, *RSC Adv.* 6, 74453 (**2016**).
3. W. Wang, Y. Xie, Y. Wang, H. Du, C. Xia, and F. Tian, *Microchim. Acta* 181, 381 (**2014**).
4. B. Kowalewska and K. Jakubow, *Sens. Actuators B Chem.* 238, 852 (**2017**).
5. M. ElKaoutit, I. N. Rodriguez, M. Dominguez, and J. L. H. H. Cisneros, *Appl. Surf. Sci.* 257, 10926 (**2011**).
6. M. Senel, M. Dervisevic, and E. Çevik, *Curr. Appl. Phys.* 13, 1199 (**2013**).

7. P. D. Gaikwad, D. J. Shirale, V. K. Gade, P. A. Savale, H. J. Kharat, K. P. Kakde, and M. D. Shirsat, *Int. J. Electrochem. Sci.* 1, 425 (**2006**).
8. M. Z. Cetin and P. Camurlu, *J. Electrochem. Soc.* 164, B585 (**2017**).
9. W. Huang, Q. Hao, W. Lei, L. Wu, and X. Xia, *Mater. Res. Express* 1, 045601 (**2014**).
10. M. Grzeszczuk and R. Ozsakary, *RSC Adv.* 4, 22214 (**2014**).
11. P. A. Palod and V. Singh, *Mater. Sci. Eng. C* 55, 420 (**2015**).
12. A. Fakhry, F. Pillier, and C. D. Chouvy, *J. Mater. Chem. A* 2, 9859 (**2014**).
13. P. A. Palod and V. Singh, *Sens. Actuators B Chem.* 209, 85 (**2015**).
14. X. H. Chu, Q. Xu, Z. Q. Feng, J. Q. Xiao, Q. Li, X. T. Sun, Y. Cao, and Y. T. Ding, *Mater. Res. Express* 1, 035402 (**2014**).
15. E. Tavakkola, H. Tavanaia, A. Abdolmalekib, and M. Morshed, *Synthetic Met.* 231, 95 (**2017**).
16. J. Zang, C. M. Li, S. J. Bao, X. Cui, Q. Bao, and C. Q. Sun, *Macromolecules* 41, 7053 (**2008**).
17. A. Keyhanpour, S. M. S. Mohaghegh, and A. Jamshidi, *Biosens Bioelectron* 3, 1 (**2012**).
18. X. Zhang, D. Liu, L. Li, and T. You, *Sci. Rep.* 5, 09885 (**2015**).
19. O. Çolak, A. Yaşar, S. Çete, and F. Arslan, *Artif. Cells Blood Subst. Biotechnol.* 40, 354 (**2012**).
20. J. Shi, J. C Claussen, E. S McLamore, A. ul Haque, D. Jaroch, A. R Diggs, P. C. Marzal, J. L Rickus, and D. M. Porterfield, *Nanotechnol.* 22, 355502 (**2011**).
21. Y. Xie and Y. Zhao, *Mater. Sci. Eng. C* 33, 5028 (**2013**).
22. M. Shukla, Pramila, I. A. Palani, and V. Singh, *J. Phys.: Conf. Ser.* 924, 012013 (**2017**).
23. P. Jakhar, M. Shukla, and V. Singh, *J. Electrochem. Soc.* 165, G80 (**2018**).
24. P. A. Palod, S. S. Pandey, S. Hayase, and V. Singh, *Appl. Biochem. Biotechnol.* 174, 1059 (**2014**).
25. M. Shukla, Pramila, J. Agrawal, T. Dixit, I.A. Palani, and V. Singh, *Mater. Res. Express* 5, 055031 (**2018**).
26. B. K. Shrestha, R. Ahmad, S. Shrestha, C. H. Park, and C. S. Kim, *Sci. Rep.* 7, 16191 (**2017**).
27. X. Xu, P. Wu, W. Xu, Q. Shao, L. An, H. Zhang, C. Cai, and B. Zhao, *Phys. Chem. Chem. Phys.* 14, 5824 (**2012**).
28. W. Tang, L. Li, L. Wu, J. Gong, and X. Zeng, *PLOS ONE* 9, e95030 (**2014**).
29. M. Yan, D. Zang, S. Ge, L. Ge, and J. Yu, *Biosens Bioelectron* 38, 355 (**2012**).
30. Y. M. Uang and T. C. Chou, *Biosens Bioelectron* 19, 141 (**2003**).
31. M. Shukla, Pramila, T. Dixit, I. A. Palani, and V. Singh, *Appl. Surf. Sci.* 422, 798 (**2017**).
32. K. Anderson, B. Poulter, J. Dudgeon, S.-E. Li, and X. Ma, *Sensors* 17, 1807 (**2017**).
33. D. Bruen, C. Delaney, L. Florea, and D. Diamond, *Sensors* 17, 1866 (**2017**).
34. F. L. Gallego, L. Betancor, C. Mateo, A. Hidalgo, N. A. Morales, G. D. Ortiz, J. M. Guisan, R. F. Lafuente, *J. Biotechnol*. 119, 70 (**2005**).

Received: 9 August 2018. Accepted: 24 December 2018.